

Selectivity as a Function of Nanoparticle Size in the Catalytic Hydrogenation of Unsaturated Alcohols

Somnath Bhattacharjee, David M. Dotzauer, and Merlin L. Bruening*

Department of Chemistry, Michigan State University, East Lansing, Michigan 48824

Received September 18, 2008; E-mail: bruening@chemistry.msu.edu

Abstract: Layer-by-layer adsorption of poly(acrylic acid)–Pd(II) complexes and poly(ethylenimine) on alumina powder followed by reduction of Pd(II) with NaBH₄ yields Pd–nanoparticle catalysts embedded in multilayer polyelectrolyte films. The use of different ratios of poly(acrylic acid) to Pd(II) in deposition solutions gives a series of films with Pd nanoparticles whose average diameters range from 2.2 to 3.4 nm, and the catalytic selectivities of these nanoparticles vary dramatically with their size. Turnover frequencies (TOFs) for the hydrogenation of monosubstituted unsaturated alcohols increase with decreasing average nanoparticle size, whereas multisubstituted unsaturated alcohols show the opposite trend. Hence, the ratio of TOFs for the hydrogenation of allyl alcohol and crotyl alcohol is 39 with average particle diameters of 2.2 nm and only 1.3 with average particle diameters of 3.4 nm. Ratios of TOFs for hydrogenation of allyl alcohol and β -methallyl alcohol are as high as 240 with the smallest nanoparticles, but substantial isomerization of β -methallyl alcohol complicates this comparison. Increasing selectivity with decreasing average particle size occurs with both films deposited on alumina powder and nanoparticles stabilized by polyelectrolytes in solution. Presumably, high selectivities occur on the smallest nanoparticles because the active sites on the smallest Pd nanoparticles are less available for binding and hydrogenation of multisubstituted double bonds than are active sites on larger particles.

Introduction

Control over particle size is essential in creating highly active nanoparticle catalysts for alkene hydrogenation,^{1–5} alcohol oxidation,^{6,7} Suzuki⁸ and Heck⁹ coupling, Norrish type II reactions,¹⁰ reduction of aromatic nitro compounds,¹¹ CO oxidation,^{12,13} and electrooxidation of formic acid^{14,15} and methanol.¹⁶ Nanoparticle size is also a critical parameter for achieving partial hydrogenation in the conversion of alkynes

to alkenes,^{17,18} α,β unsaturated aldehydes to unsaturated alcohols,¹⁹ and conjugated alkenes to monoalkenes.^{20,21} Moreover, nanoparticle catalysts show high intermolecular selectivities in the hydrogenation of alkenes²² and allylic alcohols,^{23–27} but selectivity has not been studied as a function of particle size. Examination of selectivities is particularly attractive for understanding the effect of particle size on reactivity because rate enhancements due solely to increases in surface area should cancel when calculating the ratios of reaction rates for structurally related compounds.

This study shows that both the rates and the selectivities of hydrogenation reactions vary dramatically with the diameter of catalytic nanoparticles. Remarkably, in the hydrogenation of mono- and disubstituted double bonds nanoparticles with average diameters of 2.2 nm exhibit selectivities as high as 39

- (1) Wilson, O. M.; Knecht, M. R.; Garcia-Martinez, J. C.; Crooks, R. M. *J. Am. Chem. Soc.* **2006**, *128*, 4510–4511.
- (2) Doyle, A. M.; Shaikhutdinov, S. K.; Freund, H.-J. *Angew. Chem., Int. Ed.* **2005**, *44*, 629–631.
- (3) Doyle, A. M.; Shaikhutdinov, S. K.; Jackson, S. D.; Freund, H.-J. *Angew. Chem., Int. Ed.* **2003**, *42*, 5240–5243.
- (4) Xu, B.; Liew, K. Y.; Li, J. *J. Am. Oil Chem. Soc.* **2007**, *84*, 117–122.
- (5) Shaikhutdinov, S.; Heemeier, M.; Baumer, M.; Lear, T.; Lennon, D.; Oldman, R. J.; Jackson, S. D.; Freund, H. J. *J. Catal.* **2001**, *200*, 330–339.
- (6) Chen, J.; Zhang, Q.; Wang, Y.; Wan, H. *Adv. Synth. Catal.* **2008**, *350*, 453–464.
- (7) Li, F.; Zhang, Q.; Wang, Y. *Appl. Catal., A* **2008**, *334*, 217–226.
- (8) Li, Y.; Boone, E.; El-Sayed, M. A. *Langmuir* **2002**, *18*, 4921–4925.
- (9) Le Bars, J.; Specht, U.; Bradley, J. S.; Blackmond, D. G. *Langmuir* **1999**, *15*, 7621–7625.
- (10) Kell, A. J.; Donkers, R. L.; Workentin, M. S. *Langmuir* **2005**, *21*, 735–742.
- (11) Panigrahi, S.; Basu, S.; Praharaj, S.; Pande, S.; Jana, S.; Pal, A.; Ghosh, S. K.; Pal, T. *J. Phys. Chem. C* **2007**, *111*, 4596–4605.
- (12) Valden, M.; Lai, X.; Goodman, D. W. *Science* **1998**, *281*, 4.
- (13) Overbury, S. H.; Schwartz, V.; Mullins, D. R.; Yan, W.; Dai, S. J. *Catal.* **2006**, *241*, 56–65.
- (14) Zhou, W. P.; Lewera, A.; Larsen, R.; Masel, R. I.; Bagus, P. S.; Wieckowski, A. *J. Phys. Chem. B* **2006**, *110*, 13393–13398.
- (15) Zhou, W.; Lee, J. Y. *J. Phys. Chem. C* **2008**, *112*, 3789–3793.
- (16) Bergamaski, K.; Pinheiro, A. L. N.; Teixeira-Neto, E.; Nart, F. C. J. *Phys. Chem. B* **2006**, *110*, 19271–19279.

- (17) Semagina, N.; Renken, A.; Laub, D.; Kiwi-Minsker, L. *J. Catal.* **2007**, *246*, 308–314.
- (18) Semagina, N.; Renken, A.; Kiwi-Minsker, L. *J. Phys. Chem. C* **2007**, *111*, 13933–13937.
- (19) Claus, P.; Brueckner, A.; Mohr, C.; Hofmeister, H. *J. Am. Chem. Soc.* **2000**, *122*, 11430–11439.
- (20) Tardy, B.; Noupa, C.; Leclercq, C.; Bertolini, J. C.; Hoareau, A.; Treilleux, M.; Faure, J. P.; Nihoul, G. *J. Catal.* **1991**, *129*, 1–11.
- (21) Silvestre-Albero, J.; Rupprechter, G.; Freund, H.-J. *J. Catal.* **2006**, *240*, 58–65.
- (22) Vasylyev, M. V.; Maayan, G.; Hovav, Y.; Haimov, A.; Neumann, R. *Org. Lett.* **2006**, *8*, 5445–5448.
- (23) Bhattacharjee, S.; Bruening, M. L. *Langmuir* **2008**, *24*, 2916–2920.
- (24) Kidambi, S.; Dai, J.; Li, J.; Bruening, M. L. *J. Am. Chem. Soc.* **2004**, *126*, 2658–2659.
- (25) Kidambi, S.; Bruening, M. L. *Chem. Mater.* **2005**, *17*, 301–307.
- (26) Oh, S.-K.; Niu, Y.; Crooks, R. M. *Langmuir* **2005**, *21*, 10209–10213.
- (27) Niu, Y.; Yeung, L. K.; Crooks, R. M. *J. Am. Chem. Soc.* **2001**, *123*, 6840–6846.

for allyl alcohol over crotyl alcohol, whereas nanoparticles with average diameters of 3.4 nm show corresponding selectivities less than 1.3. Such variations in selectivity occur with polymer-encapsulated nanoparticles immobilized on alumina as well as polymer-capped nanoparticles in solution.

The first step in examining the effect of nanoparticle size on catalytic activity is development of a method to synthesize nanoparticle catalysts with several different average particle sizes and narrow size distributions. Among the methods for controlling nanoparticle size, a number of studies demonstrate that layer-by-layer deposition of polyelectrolyte films containing metal ions and subsequent reduction of these metal ions provide a straightforward technique for creating encapsulated nanoparticles.^{23–25,28–32} The amount of metal ion present during film deposition dictates the particle size, and layer-by-layer deposition on micrometer-sized alumina provides heterogeneous catalysts. Polyelectrolyte–nanoparticle catalysts can also form in solution, which allows comparison of particle-size effects in supported films and solution-based catalysts.

Palladium nanoparticles in polyelectrolyte films are particularly attractive for investigating relationships between particle size and reactivity/selectivity because they show high selectivity in the hydrogenation of unsaturated alcohols.^{23,24} Previously we prepared Pd nanoparticles encapsulated in multilayer polyelectrolyte films through layer-by-layer adsorption of poly(acrylic acid) (PAA) and poly(ethylenimine)–Pd(II) (PEI–Pd(II)) complexes and reduction of Pd(II) with NaBH₄. Transmission electron microscopy confirmed formation of Pd nanoparticles, and the selectivities of [PAA/PEI–Pd(0)]₃PAA films in the hydrogenation of monosubstituted over multisubstituted double bonds were as high as 100.²³ However, we employed only one average particle size. This work examines the hydrogenation of a series of unsaturated alcohols using nanoparticle/polyelectrolyte catalysts with several average nanoparticle sizes and shows that selectivity is an extremely sensitive function of particle diameter.

Experimental Section

Materials. Poly(ethylenimine) (PEI, $M_w = 25\,000$ Da), poly(acrylic acid) (PAA, $M_w = 90\,000$ Da), α -alumina (100 mesh, typical particle size 75–100 μm), allyl alcohol (99.0%), crotyl alcohol (97.0%, mixture of isomers), 2-methyl-2-propen-1-ol (98.0%), 3-methyl-2-buten-1-ol (99.0%), propionaldehyde, 3-methyl-1-butanol (98.5+%), isovaleraldehyde (97.0%), isobutyraldehyde (98.0%), 3-methyl-1-penten-3-ol (99.0%), 3-methyl-3-pentanol (99.0%), *cis*-3-hepten-1-ol ($\geq 95.0\%$), potassium tetrachloropalladate(II) (99.99%), and sodium borohydride (98%) were purchased from Aldrich. 1-Heptanol and 3-buten-1-ol were obtained from TCI, and butyraldehyde ($\geq 99.0\%$) was purchased from Fluka. 1-Butanol (J.T. Baker), *n*-propyl alcohol (Columbus Chemical), isobutyl alcohol (Spectrum), and ethanol (100%, Pharmco) were used as received. Aqueous solutions were prepared with deionized water (18.2 M Ω cm, Milli-Q purification system), and hydrogen (99.9%) was obtained from AGA gases.

Preparation of Pd Nanoparticles Encapsulated in Polyelectrolytes. PAA–Pd(0)/PEI on Alumina. Preparation of PAA/PEI–Pd(0) films on alumina was described previously,^{23,24} and

formation of PAA–Pd(0)/PEI films occurred similarly. Alumina was alternately suspended for 10 min in a solution that contained 20 mM PAA and 1, 4, 8, or 15 mM K₂PdCl₄ and for 10 min in a solution that contained PEI (1 mg/mL). (The molarity of PAA is given with respect to the repeating unit.) Prior to their use in multilayer assembly, the PAA solution was adjusted to pH 4.0 with 0.1 M NaOH, and the PEI solution was adjusted to pH 9.0 with 0.1 M HCl. After deposition of each polyelectrolyte layer the alumina was allowed to settle, the supernatant was decanted, and the solid was suspended similarly (vigorous stirring) in three 100 mL aliquots of deionized water for 5 min to remove excess polyelectrolyte. Overall, three PAA–Pd(II)/PEI bilayers were deposited. Reduction to Pd(0) was performed by stirring the [PAA–Pd(II)/PEI]₃ films on alumina in 100 mL of freshly prepared 0.1 mM NaBH₄ for 30 min followed by washing with three 100 mL aliquots of deionized water for 5 min each. After decanting the final water rinse the residual water was removed under reduced pressure overnight to afford a catalytic powder.

Pd(0)/PEI on Alumina. [Pd(0)/PEI]₃ films on alumina were prepared as described previously.²⁵ In brief, 15 g of α -alumina powder was stirred for 30 min in 100 mL of a solution that contained K₂PdCl₄ (1 or 15 mM) and 0.1 M KCl. The alumina was washed as described above prior to suspension in PEI (2 mg/mL PEI, pH adjusted to 9.0 with 0.1 M HCl) for 10 min and additional washing. After deposition of three PdCl₄²⁻/PEI bilayers, reduction of Pd(II) to Pd(0) was performed as described above.

PAA–Pd(0)/PEI in Solution. PAA–Pd(II) was prepared by mixing 20 mM PAA and K₂PdCl₄ (1, 4, 8, or 15 mM) and adjusting the pH of the solution to 4 with 0.1 M NaOH. A 5 mL amount of this solution and 5 mL of PEI solution (1 mg/mL PEI, pH adjusted to 9.0 with 0.1 M HCl) were mixed together in a 20 mL glass vial at which point the solution became cloudy. Freshly prepared 0.1 M NaBH₄ (5 mL) was added to the cloudy PAA–Pd(II)/PEI, which was then stirred vigorously for 3 h in a loosely capped vial. The resulting clear, brown solution was then immediately used for hydrogenation.

Crooks et al. previously reported that dendrimer-encapsulated Pd nanoparticles, a homogeneous catalytic system, are unstable in the presence of oxygen.³⁵ We also observed that the brown color of the PAA–Pd(0)/PEI solution faded to pale yellow over 24 h if the solution was not capped tightly and refrigerated. This was especially apparent when the concentration of Pd(II) in the deposition solution was 1 mM.

Characterization of Pd Nanoparticles. For TEM imaging, films were deposited on carbon-coated copper grids that were pretreated in a UV/ozone cleaner for 1 min. [PAA–Pd(0)]/PEI₃ and reduced [PdCl₄²⁻/PEI]₃ films were formed as described above except the grid was simply immersed for 5 min in deposition solutions without stirring, and rinsing between each step consisted of a 1 min washing with deionized water.

To characterize the PAA–Pd(0)/PEI solutions prepared with different initial concentrations of Pd(II) (1, 4, 8, 15 mM), we first diluted the reduced solutions with sufficient deionized water to obtain 0.33 mM Pd. We then spotted a drop of these solutions on separate carbon-coated copper grids that had been pretreated with UV/ozone for 1 min and allowed the solutions to dry at room temperature overnight. Imaging was performed on a JEM-2200FS microscope using an accelerating voltage of 200 kV. Diameters of at least 250 particles for each sample were measured manually on digital images, and uncertainties in average particle diameters represent standard deviations.

The amounts of palladium in different catalysts were determined by atomic emission spectroscopy (AES). Standard solutions (0.1–0.5 mM) were prepared by dissolving K₂PdCl₄ in 0.1 M HNO₃, and sample solutions were prepared by stirring the desired amount of alumina-supported catalyst (60–500 mg, depending on the Pd

(28) Schmitt, J.; Decher, G.; Dressick, W. J.; Brandow, S. L.; Geer, R. E.; Shashidhar, R.; Calvert, J. M. *Adv. Mater.* **1997**, *9*, 61–65.

(29) Mamedov, A. A.; Belov, A.; Giersig, M.; Mamedova, N. N.; Kotov, N. A. *J. Am. Chem. Soc.* **2001**, *123*, 7738–7739.

(30) Wang, T. C.; Rubner, M. F.; Cohen, R. E. *Chem. Mater.* **2003**, *15*, 299–304.

(31) Joly, S.; Kane, R.; Radzilowski, L.; Wang, T.; Wu, A.; Cohen, R. E.; Thomas, E. L.; Rubner, M. F. *Langmuir* **2000**, *16*, 1354–1359.

(32) Wang, T. C.; Rubner, M. F.; Cohen, R. E. *Langmuir* **2002**, *18*, 3370–3375.

(33) Scott, R. W. J.; Ye, H.; Henriquez, R. R.; Crooks, R. M. *Chem. Mater.* **2003**, *15*, 3873–3878.

Table 1. Amounts and Pd Contents of Catalysts Used in Hydrogenation Reactions

catalyst	amount of catalyst	μmol of Pd in the catalyst
[PAA–Pd(0)/PEI] ₃ on Al ₂ O ₃ (Pd(II) = 1 mM), catalyst A	500 mg	1.91
[PAA–Pd(0)/PEI] ₃ on Al ₂ O ₃ (Pd(II) = 4 mM), catalyst B	250 mg	4.15
[PAA–Pd(0)/PEI] ₃ on Al ₂ O ₃ (Pd(II) = 8 mM), catalyst C	125 mg	7.66
[PAA–Pd(0)/PEI] ₃ on Al ₂ O ₃ (Pd(II) = 15 mM), catalyst D	125 mg	12.8
[PAA–Pd(0)/PEI] ₃ (PAA/PEI) ₃ on Al ₂ O ₃ (Pd(II) = 1 mM), catalyst E	500 mg	1.18
[PAA–Pd(0)/PEI] ₃ (PAA/PEI) ₃ on Al ₂ O ₃ (Pd(II) = 8 mM), catalyst F	125 mg	7.66
reduced [PdCl ₄ ²⁻ /PEI] ₃ on Al ₂ O ₃ (Pd(II) = 1 mM), catalyst G	250 mg	3.71
reduced [PdCl ₄ ²⁻ /PEI] ₃ on Al ₂ O ₃ (Pd(II) = 15 mM), catalyst H	100 mg	11.0
PAA–Pd(0)/PEI solution (Pd(II) = 1 mM), catalyst I	5.00mL	1.67
PAA–Pd(0)/PEI solution (Pd(II) = 4 mM), catalyst J	5.00mL	6.65
PAA–Pd(0)/PEI solution (Pd(II) = 8 mM), catalyst K	3.00mL	8.00
PAA–Pd(0)/PEI solution (Pd(II) = 15 mM), catalyst L	3.00mL	15.00

content) in 2 mL of aqua regia for 15 min. The aqua regia solutions were diluted to 12 mL with water and centrifuged (the α -alumina support does not dissolve in aqua regia), and the supernatant was analyzed using its emission at 340.5 nm. Table 1 lists the amounts of Pd in each of the different catalysts. For the PAA–Pd(0)/PEI solutions the amount of Pd(0) was calculated by assuming total conversion of Pd(II) to Pd(0).

Hydrogenation Reactions. Catalytic hydrogenation was performed in a 100 mL, three-neck, round-bottomed flask. Suspended alumina-supported catalyst in 25 mL of H₂O (or 25 mL of diluted catalyst solution in the case of nanoparticles stabilized by polyelectrolytes in solution) was bubbled with H₂ for 30 min before adding 25 mL of a 50 mM solution of substrate in water or in a 1:1 (v:v) mixture of ethanol, methanol, or THF and water. During the reaction, hydrogen at a gauge pressure of 50 kPa was bubbled through a frit at the bottom of a solution that was vigorously stirred. Different amounts of catalyst (Table 1) were used for hydrogenation reactions because each type of material has a different wt % of Pd. Aliquots of 0.5 mL were removed from the reaction vessel at specific times, filtered with cotton to remove the catalyst, and diluted by addition of 1 mL deionized water prior to analysis by gas chromatography (Shimadzu GC-17A equipped with an RTx-BAC1 column). In the GC analysis of hydrogenation of **3**, product and reactant peaks showed a small overlap, and one limit of integration was placed at the minimum between the peaks. Response factors were determined to calculate the turnover frequency (TOF) as described previously.²³ TOFs were calculated from the slope of the initial portion (total conversion of reactant to isomer and hydrogenated product < 50%) of plots of percent hydrogenation versus time. In fitting the initial data the intercept of the line was

forced through zero. Each experiment was repeated twice, and the \pm values represent the difference between the average and the data points.

Results and Discussion

Catalyst Synthesis and Variation of Particle Size. The initial step in studying the effect of nanoparticle size on catalytic selectivity is to prepare a series of catalysts with different particle sizes. Previously, we made [PAA/PEI–Pd(II)]₃PAA films using 2 mM Pd(II) in the PEI–Pd(II) deposition solution. Subsequent reduction of the Pd(II) gave [PAA/PEI–Pd(0)]₃PAA coatings containing Pd nanoparticles with diameters of 1–3 nm.²³ We tried to enhance nanoparticle size by increasing the concentration of Pd(II) in the PEI deposition solution, but at a Pd(II) concentration of 12 mM, the PEI solution became cloudy, perhaps because the Pd(II) serves as a cross-linking agent for PEI chains. To overcome this challenge, we added Pd(II) to the PAA, rather than PEI, deposition solution. The 20 mM PAA deposition solution (PAA concentration is given with respect to the repeating unit) remains clear at Pd(II) concentration as high as 15 mM. Prior studies demonstrated deposition of metal ions in PAA/protonated poly(allylamine) films and subsequent formation of nanoparticles,^{31,32} but in the present case we add the metal ions during film formation.

Most importantly, reduction of [PAA–Pd(II)/PEI]₃ using NaBH₄ yields [PAA–Pd(0)/PEI]₃ films, and the sizes of the resulting Pd nanoparticles increase with increasing concentrations of Pd(II) in PAA deposition solutions. Figures 1 and 2 as well as Figures S-1 and S-2 of the Supporting Information present TEM images of films on carbon-coated grids and histo-

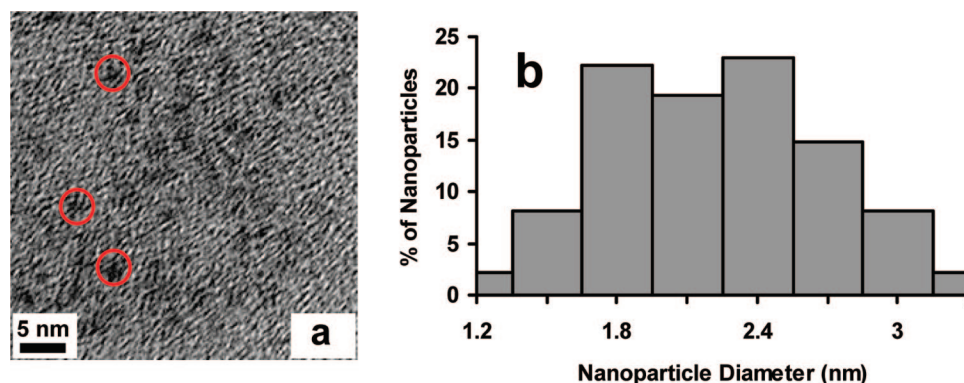


Figure 1. (a) TEM image of a [PAA–Pd(0)/PEI]₃ film on a carbon-coated copper grid. One millimolar Pd(II) was present in the PAA–K₂PdCl₄ solution used for film deposition. A few of the nanoparticles are circled. (b) Histogram of Pd nanoparticle diameters in several TEM images. The average particle size is 2.2 \pm 0.6 nm. The area-average particle size is 2.5 \pm 0.7 nm.

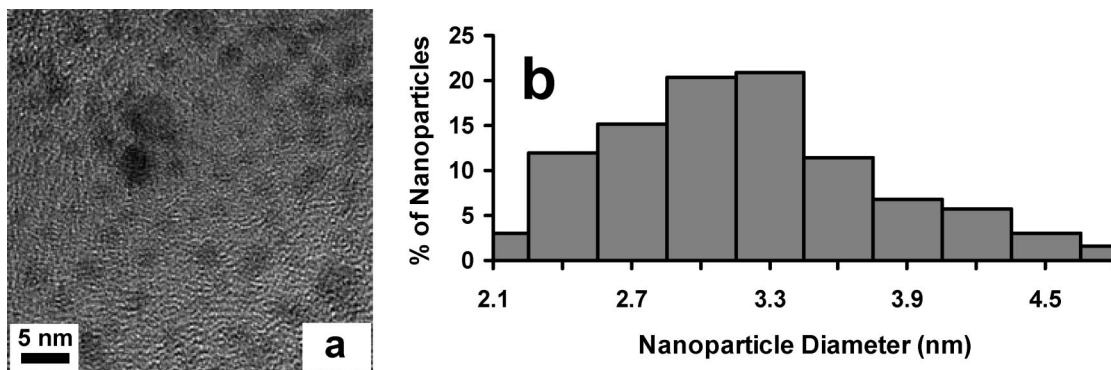


Figure 2. (a) TEM image of a [PAA–Pd(0)/PEI]₃ film on a carbon-coated copper grid. Eight millimolar Pd(II) was present in the PAA–K₂PdCl₄ solution used for film deposition. (b) Histogram of Pd nanoparticle diameters in several TEM images. The average particle size is 3.2 ± 0.6 nm. The area-average particle size is 3.5 ± 0.7 nm.

grams of particle size. With Pd(II) concentrations of 1, 4, 8, or 15 mM in the PAA deposition solutions, the average particle diameters in [PAA–Pd(0)/PEI]₃ films on TEM grids are 2.2 ± 0.6, 2.9 ± 0.5, 3.2 ± 0.6, and 3.4 ± 0.9 nm, respectively. Area-average particle sizes might be more representative of catalytic activities because larger particles make up a disproportionate share of the total catalyst surface area. We calculate the area-average diameters, D_A , using eq 1, where D_i represents the diameters of individual particles.

$$D_A = \frac{\sum_i D_i D_i^2}{\sum_i D_i^2} \quad (1)$$

Values of D_A are 2.5 ± 0.7, 3.1 ± 0.5, 3.5 ± 0.7, and 3.8 ± 1.1 nm for films prepared using 1, 4, 8, and 15 mM Pd(II), respectively, in the 20 mM PAA deposition solutions. We should note that some particles with diameters less than 2 nm may be present but not visible.

Occasionally, TEM images of [PAA–Pd(0)/PEI]₃ films prepared with 15 mM Pd(II) in the PAA deposition solutions exhibit areas containing large particles with average diameters of 160 ± 100 nm (Figure S-3a, Supporting Information). We did not include these larger particles in the calculation of average particle diameters because they constitute only about 18% of the total particle surface area (Table S-1, Supporting Information), and we are not sure whether they are representative of all samples. However, the absolute values of TOFs for catalysis with alumina-supported [PAA–Pd(0)/PEI]₃ films that are prepared using 15 mM Pd(II) should be viewed with caution.

Although we use films deposited on alumina particles for catalysis, we perform the TEM analyses with films on carbon-coated Cu grids because it is very difficult to visualize nanoparticles on the rough alumina microparticles. The nanoparticles likely have similar diameters on the TEM grids and on the alumina, but we cannot verify the diameters of particles on alumina. To address this problem, we also prepare polyelectrolyte/nanoparticle composites in water. These materials serve as catalysts and are amenable to TEM imaging, which allows a direct correlation between catalytic activity and particle size. A recent study showed that in many cases nanoparticles in water do not aggregate in the presence of polyelectrolytes.³⁴

Preparation of the suspended polyelectrolyte/nanoparticle composites includes addition of an aqueous solution of PEI (1 mg/mL, pH adjusted to 9) to a solution of PAA (20 mM, pH adjusted to 4) that contains various concentrations of K₂PdCl₄ (1, 4, 8, or 15 mM). The yellow-colored PAA–Pd(II) solution becomes cloudy after addition of PEI and then turns to a clear brown color after addition of 0.1 M aqueous NaBH₄ and vigorous stirring. The pH of the PAA–Pd(II)/PEI mixture is about 5, but addition of 0.1 M NaBH₄ gives a clear solution with a pH of ~9. Raising the pH of PAA–Pd(II)/PEI solutions by addition of 0.1 M NaOH also yields a clear solution, presumably because less protonation of PEI results in weaker PAA/PEI complexes. However, both polyelectrolytes are important for stabilizing the nanoparticles. Addition of 0.1 M NaBH₄ to solutions containing either PAA and 8 mM Pd(II) or PEI and 8 mM Pd(II) produces a black precipitate.

To determine the sizes of nanoparticles suspended in these solutions, we deposit a drop of solution on a carbon-coated copper grid and then image the nanoparticles with TEM. These TEM images along with histograms of particle sizes (Figures 3, 4, S-4, and S-5, Supporting Information) indicate formation of nanoparticles whose size is a function of the concentration of Pd(II) in solution prior to reduction. In this case, the average particle diameters that result from the use of 1, 4, 8, and 15 mM Pd(II) to form nanoparticles are 2.6 ± 0.8, 3.2 ± 0.7, 3.5 ± 0.7 and 5.1 ± 1.3 nm, respectively. Corresponding area-average diameters are 3.1 ± 0.8, 3.4 ± 0.7, 3.7 ± 0.7, and 5.8 ± 1.4 nm. We do not observe any large (>9 nm) particles in PAA–Pd(0)/PEI solutions prepared with Pd(II) concentrations of 15 mM in the PAA deposition solutions (Figure S-6, Supporting Information).

Selective Hydrogenation with Films on Alumina Particles.

To investigate catalytic selectivity as a function of nanoparticle diameter we first hydrogenated allyl alcohol (**1**, a monosubstituted unsaturated alcohol), 2-methyl-2-propen-1-ol (**2**, a disubstituted unsaturated alcohol), and crotyl alcohol (**3**, a disubstituted unsaturated alcohol) in separate solutions. TOFs (mol hydrogenated/mol Pd/h) at low substrate conversion provide a quantitative comparison of the reactivities and selectivities of the different catalysts. Unfortunately, interpretation of the TOFs is complicated by isomerization of the unsaturated alcohols to the corresponding aldehydes, which are not readily hydrogenated. Thus, Table 2 contains TOFs for initial hydrogenation along with values in parentheses that reflect the sum of the initial hydrogenation and initial isomerization TOFs. Isomerization is most extensive for **2**, presumably because its isomer is a

(34) Rouhana, L. L.; Jaber, J. A.; Schlenoff, J. B. *Langmuir* **2007**, *23*, 12799–12801.

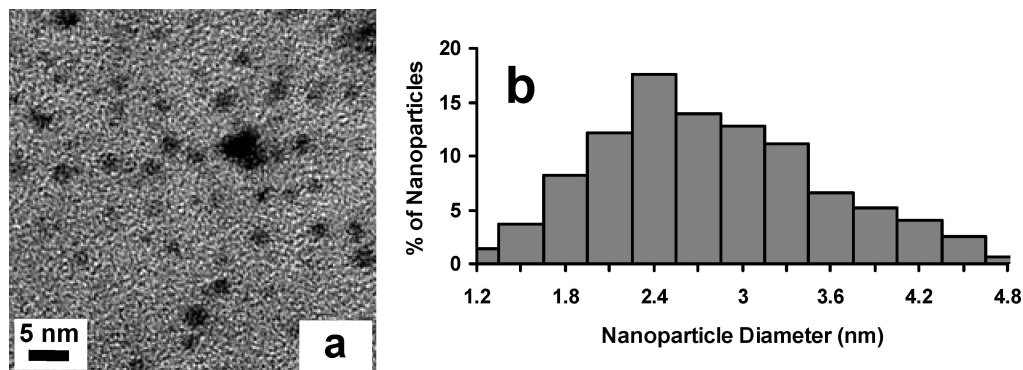


Figure 3. (a) TEM image of a dried PAA–Pd(0)/PEI solution on a carbon-coated copper grid. One millimolar Pd(II) was initially present in the PAA solution. (b) Histogram of Pd nanoparticle diameters in several TEM images. The average particle size is 2.6 ± 0.8 nm. The area-average particle size is 3.1 ± 0.8 nm.

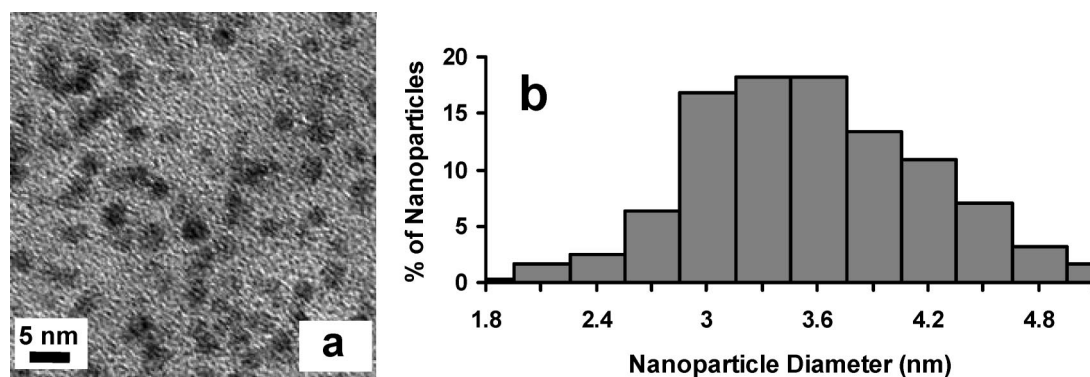
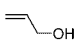
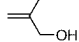
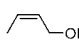


Figure 4. (a) TEM image of a dried PAA–Pd(0)/PEI solution on a carbon-coated copper grid. Eight millimolar Pd(II) was initially present in the PAA solution. (b) Histogram of Pd nanoparticle diameters in several TEM images. The average particle size is 3.5 ± 0.7 nm. The area-average particle size is 3.7 ± 0.7 nm.

Table 2. TOFs and TOF Ratios for Unsaturated–Alcohol Hydrogenation Catalyzed by [PAA–Pd(0)/PEI]₃ Films That Contain Pd Nanoparticles with Different Diameters (catalytic films were deposited on micrometer-sized alumina; values in parentheses are the sum of TOFs for hydrogenation and isomerization)

Catalyst	Average nano-particle diameter (nm)	TOFs (moles hydrogenated/ mol Pd/ h) ^a			Ratio of TOFs	
					1/2	1/3
		1	2	3		
Catalyst A [Pd(II)]=1 mM ^b	2.2	2900±570 (6200±2400)	12±1 (85±5)	75±15 (85±15)	240 (73)	39 (73)
Catalyst B [Pd(II)]=4 mM ^b	2.9	1700±830 (4100±1800)	160±10 (730±20)	450±80 (620±130)	11 (5.6)	3.8 (6.6)
Catalyst C [Pd(II)]=8 mM ^b	3.2	1100±300 (2400±800)	165±5 (895±15)	610±60 (760±80)	6.7 (2.7)	1.8 (3.2)
Catalyst D [Pd(II)]=15 mM ^b	3.4	760±40 (2050±80)	290±70 (1400±100)	580±100 (790±160)	2.6 (1.5)	1.3 (2.6)

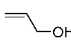
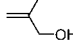
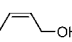
^a A 50 mL amount of 25 mM substrate was hydrogenated in water. TOFs are initial values determined at conversions less than 50%. ^b Initial concentration of K₂PdCl₄ in the PAA deposition solutions.

trisubstituted unsaturated alcohol that is more stable than **2** and readily tautomerizes to the corresponding aldehyde.

Table 2 shows that regardless of nanoparticle size, both the TOF for hydrogenation and the combined hydrogenation/isomerization TOF are higher for **1** than for **2** or **3**, which contain disubstituted double bonds. In addition, selectivity varies dramatically with the particle size. The general trend in Table 2 is that the rate of hydrogenation of **1** (column 3) decreases

with increasing nanoparticle size, while the corresponding TOFs for **2** (column 4) and **3** (column 5) increase with increasing nanoparticle size, even though the surface area to volume ratio for the catalyst is smaller for larger particles. Most remarkably, this trend yields selectivities (ratios of TOFs for different compounds, columns 6 and 7 of Table 2) that are as much as 90-fold larger with the smallest nanoparticles than with the largest. These trends also hold when considering the sum of

Table 3. TOFs and TOF Ratios for Unsaturated-Alcohol Hydrogenation Catalyzed by [PAA–Pd(0)/PEI]₃/(PAA/PEI)₃ Films That Contain Pd Nanoparticles with Different Diameters (films were deposited on micrometer-sized alumina; values in parentheses are the sum of TOFs for hydrogenation and isomerization)

Catalyst	Average nano-particle diameter (nm)	TOFs (moles hydrogenated/ mol Pd/ h) ^a			Ratio of TOFs	
					1/2	1/3
		1	2	3		
Catalyst E [Pd(II)]=1 mM ^b	2.2	1500±250 (3000±1000)	10±1 (40±5)	35±5 (40±5)	150 (75)	43 (75)
Catalyst F [Pd(II)]=8 mM ^b	3.2	650±20 (1160±50)	80±15 (300±50)	190±10 (250±10)	8.1 (3.9)	3.4 (4.6)

^a 25 mM substrate was hydrogenated in water. TOFs are initial values determined at conversions less than 50%. ^b Initial concentration of K₂PdCl₄ in the PAA deposition solutions.

hydrogenation and isomerization. The selectivities for **1/2** and **1/3** with the smaller nanoparticles are especially notable because Wilkinson's catalyst, the prototypical homogeneous catalyst for selective hydrogenation, shows essentially no selectivity in the hydrogenation of mono- and disubstituted double bonds.^{23,35}

Several studies show that polyelectrolyte multilayers provide a significant barrier to the diffusion of small compounds, and even molecules as small as glycerol and methanol show much slower transport than water in polyelectrolyte films.³⁶ Thus, one possible explanation for the high selectivities of nanoparticles in polyelectrolyte films is that the polyelectrolytes decrease the rate at which bulkier molecules reach catalytic sites. To examine whether simple diffusion through polyelectrolyte films enhances selectivity, we coated films containing the 2.2 and 3.2 nm diameter nanoparticles with additional layers of polyelectrolytes. Pd was reduced prior to deposition of the top three PAA/PEI bilayers. A comparison of Tables 2 and 3 shows addition of three PAA/PEI bilayers on the top of a film containing 2.2 nm diameter particles does not have a large effect on the relative TOFs of **1** and **2** or **1** and **3**, although the magnitudes of TOF values decrease by a factor of ~2. Addition of three PAA/PEI bilayers to films containing nanoparticles with a diameter of 3.2 nm increases selectivity slightly, which is likely due to the selective transport of **2** and **3** through the additional polyelectrolyte layers. However, the selectivity of these catalysts is still 18- (1/2) and 12-fold (1/3) lower than that with the 2.2 nm nanoparticles (Table 3). These data suggest that the most important factor behind selectivity is nanoparticle size.

To further demonstrate that nanoparticle size is the primary factor behind selectivity, we studied catalysis with reduced [PdCl₄²⁻/PEI]₃ coatings on alumina. (The nomenclature PdCl₄²⁻ reflects deposition conditions and not the state of Pd in the films.) These nanoparticle-containing films should be more permeable than [PAA–Pd(0)/PEI] coatings because they contain only one polyelectrolyte.²⁵ After reduction of the Pd(II) in these films, the average particle size is 3.4 ± 0.8 nm when using 15 mM PdCl₄²⁻ to prepare the films and 3.0 ± 0.9 nm when using a 1 mM PdCl₄²⁻ solution (see Figures S-7 and S-8 of the Supporting Information). Corresponding area-average diameters are 3.8 ± 0.9 and 3.5 ± 1.0 nm, respectively. In this case,

nanoparticle sizes are not very different because PdCl₄²⁻ does not bind to a polymer in solution before adsorbing to the film but rather adsorbs directly to the polyelectrolyte film. Because the amount of adsorbed PdCl₄²⁻ in PdCl₄²⁻/PEI films is somewhat self-limiting as the film becomes negatively charged, PdCl₄²⁻ concentration should not have a dramatic effect on the amount of Pd in the film. However, in some areas of reduced [PdCl₄²⁻/PEI]₃ films prepared with 15 mM Pd(II), TEM images show the presence of large particles (average particle size 170 ± 110 nm) as well as nanoparticles (Figure S-9, Supporting Information). We estimate that the large particles represent ~33% of the total Pd surface area. We did not include these larger particles in the calculation of average particle diameters because we are not sure whether they are representative of all samples. The absolute values of TOFs for catalysis with reduced [PdCl₄²⁻/PEI]₃ films that are prepared using 15 mM Pd(II) should, thus, be viewed with caution.

Table 4 summarizes the TOFs for the hydrogenation of **1**, **2**, and **3** using the two different reduced [PdCl₄²⁻/PEI] films on alumina. The smaller nanoparticles in catalyst **G** give selectivities that are an order of magnitude higher than hydrogenation using catalyst **H** even though the average nanoparticle diameters in the two catalysts differ by only 0.40 nm.

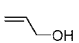
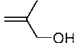
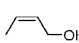
Hydrogenation with Nanoparticle/Polyelectrolyte Complexes in Solution. Because we cannot effectively image nanoparticle catalysts on alumina, we also examined hydrogenation with suspended PAA–Pd(0)/PEI catalysts prepared by addition of a PEI (1 mg/mL) solution to 20 mM PAA solutions containing different concentrations of Pd(II). Reduction of the Pd(II) with NaBH₄ yields suspended PAA–Pd(0)/PEI catalysts with a variety of Pd nanoparticle sizes. One concern when using these nanoparticles is that excess NaBH₄, which is not removed from the nanoparticle solution, might promote side reactions. As a control experiment, we attempted reduction of allyl alcohol in the absence of hydrogen gas using the PAA–Pd(0)/PEI solution containing excess NaBH₄. No reaction occurs, which rules out the possibility of NaBH₄ participating in side reactions.

Similar to catalysis by nanoparticle-containing films on alumina, with the PAA–Pd(0)/PEI solution the TOF for catalytic hydrogenation of **1** decreases with increasing particle size whereas the TOFs for **2** and **3** either increase or remain approximately constant as particle size increases (Table 5). Thus, overall selectivity shows an order of magnitude decrease on going from an average nanoparticle diameter of 2.6 to 5.1 nm. Comparison of Tables 2, 4, and 5 shows that selectivities are

(35) Takaya, H.; Noyori, R. In *Comprehensive Organic Synthesis: Selectivity, Strategy and Efficiency in Modern Organic Chemistry*; Trost, B. M., Fleming, I., Eds.; Pergamon: New York, 1991; Vol 8, pp 443–469.

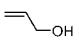
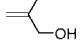
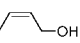
(36) Liu, X.; Bruening, M. L. *Chem. Mater.* **2004**, *16*, 351–357.

Table 4. TOFs and TOF Ratios for Unsaturated-Alcohol Hydrogenation Catalyzed by Reduced $[\text{PdCl}_4^{2-}/\text{PEI}]_3$ Films That Contain Pd Nanoparticles with Different Diameters (films were deposited on micrometer-sized alumina; values in parentheses are the sum of TOFs for hydrogenation and isomerization)

Catalyst	Average nanoparticle diameter (nm)	TOFs (moles hydrogenated/ mol Pd/ h) ^a			Ratio of TOFs	
					1/2	1/3
		1	2	3		
Catalyst G [Pd(II)]=1 mM ^b	3.0	2230±70 (4600±380)	25±5 (150±40)	220±40 (250±40)	89 (30)	10 (19)
Catalyst H [Pd(II)]=15 mM ^b	3.4	880±110 (2300±100)	380±110 (1700±350)	580±80 (750±100)	2.3 (1.4)	1.5 (3.1)

^a 25 mM substrate was hydrogenated in water. TOFs are initial values determined at conversions less than 50%. ^b Initial concentration of K_2PdCl_4 in the deposition solutions.

Table 5. TOFs and TOF Ratios for Unsaturated-Alcohol Hydrogenation Catalyzed by a Solution of PAA–Pd(0)/PEI That Contains Pd Nanoparticles with Different Diameters (values in parentheses are the sum of TOFs for hydrogenation and isomerization)

Catalyst	Average nanoparticle diameter (nm)	TOFs (moles hydrogenated/ mol Pd/ h) ^a			Ratio of TOFs	
					1/2	1/3
		1	2	3		
Catalyst I [Pd(II)]=1 mM ^b	2.6	3700±860 (5800±1900)	12 (75±5)	30±10 (35±15)	310 (73)	120 (170)
Catalyst J [Pd(II)]=4 mM ^b	3.2	1600±190 (2900±600)	12 (50±5)	45±5 (50±10)	130 (59)	35 (59)
Catalyst K [Pd(II)]=8 mM ^b	3.5	1100±560 (2400±950)	12±4 (60±5)	35±5 (45±5)	95 (40)	33 (54)
Catalyst L [Pd(II)]=15 mM ^b	5.1	890±210 (1700±350)	30±10 (100±15)	80±15 (100±15)	30 (16)	10 (18)

^a 25 mM substrate was hydrogenated in water. TOFs are initial values determined at conversions less than 50%. ^b The initial concentration of K_2PdCl_4 in the PAA deposition solutions.

frequently higher for these suspended nanoparticles than they are for $[\text{PAA}-\text{Pd}(0)/\text{PEI}]_3$ and reduced $[\text{PdCl}_4^{2-}/\text{PEI}]_3$ films on alumina. The suspended nanoparticles in solution may present a more uniform set of catalytic sites than the films on alumina powder, and uniformity might favor high selectivity. In general, supported catalysts are complex materials due to the presence of many types of potential active sites.

Solvent Effects on Hydrogenation. Previous studies of catalytic hydrogenation showed that variations in solvent can lead to changes in reaction rates, differences in the extent of double-bond isomerization, or changes in selectivity.^{23,24,27,37,38} Presumably, molecules of solvents such as MeOH, EtOH, and THF adsorb to the catalyst to alter reactivities. Additionally, swelling of polyelectrolyte films in water may increase reaction rates relative to reaction in organic solvents.³⁹ We examined hydrogenation with catalysts **A** and **D** using solvents consisting of 3 parts water and 1 part MeOH, EtOH, or THF. These two catalysts represent the widest range of particle diameters among the nanoparticles deposited on alumina.

Table 6 summarizes the TOFs for hydrogenation of **1**, **2**, and **3** in different mixed solvents. With catalyst **A** TOFs are higher in water (data in Table 2) than the mixed solvent systems (Table 6), but there is no clear trend in the different solvents. Higher swelling in water could contribute to the higher reaction rate. Table 6 also shows that with catalyst **A** selectivities are higher in 3:1 water/methanol than any of the other solvents. The small methanol molecules might more effectively compete for binding sites with **2** and **3** than with **1**. For catalyst **D** (average particle diameter of 3.4 nm), the rate of hydrogenation for all of the compounds decreases in the order water/methanol > water/ethanol > water/THF.

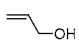
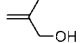
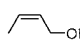
Hydrogenation of Other Unsaturated Alcohols. To examine the generality of these results, we studied the hydrogenation of several additional molecules using catalysts **A** and **D**, which have approximate nanoparticle diameters of 2.2 and 3.4 nm, respectively. As Table 7 shows, the rate of hydrogenation of compounds **4–7** decreases in the order monosubstituted double bonds > disubstituted double bond > trisubstituted double bonds. (These reactions occur in 3:1 water/ethanol to ensure substrate solubility.) Compounds **4** and **1** both contain a monosubstituted double bond, but in 3:1 water:ethanol hydrogenation of **4** by catalyst **A** occurs at a slower rate than hydrogenation of **1** (compare Tables 6 and 7). Nevertheless, the TOF for the hydrogenation of **4** is still 11 times higher than

(37) Sulman, E.; Bodrova, Y.; Matveeva, V.; Semagina, N.; Cervený, L.; Kurtc, V.; Bronstein, L.; Platonova, O.; Valetsky, P. *Appl. Catal., A* **1999**, *176*, 75–81.

(38) Augustine, R. L.; Warner, R. W.; Melnick, M. J. *J. Org. Chem.* **1984**, *49*, 4853–6.

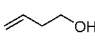
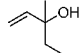
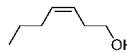
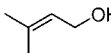
(39) Miller, M. D.; Bruening, M. L. *Chem. Mater.* **2005**, *17*, 5375–5381.

Table 6. TOFs and TOF Ratios for Unsaturated-Alcohol Hydrogenation Catalyzed by [PAA–Pd(0)/PEI]₃ Films in Different Solvents (films contain Pd nanoparticles with different diameters and are deposited on micrometer-sized alumina; values in parentheses are the sum of TOFs for hydrogenation and isomerization)

Catalysts	Solvent Mixtures	TOFs (moles hydrogenated/ mol Pd/ h) ^a			Ratio of TOFs	
					1/2	1/3
		1	2	3		
Catalyst A ^b [Pd(II)]=1 mM ^c	Water & MeOH (3:1)	1400±100 (2500±250)	4 (30±10)	15±5 (20±5)	350 (83)	93 (125)
	Water & EtOH (3:1)	1600±400 (2900±650)	6±1 (45±5)	40±5 (45±5)	267 (64)	40 (64)
	Water & THF (3:1)	600±200 (1050±50)	-	25±15 (-)	-	24 (-)
Catalyst D ^b [Pd(II)]=15 mM ^c	Water & MeOH (3:1)	1200±350 (3900±1150)	280±5 (1400±200)	700±100 (1050±200)	4.3 (2.8)	1.7 (3.7)
	Water & EtOH (3:1)	810±320 (2900±1100)	220±10 (1500±220)	400±100 (660±160)	3.7 (1.9)	2.0 (4.4)
	Water & THF (3:1)	300±60 (1300±390)	-	250±20 (-)	-	1.2 (-)

^a Several TOFs could not be estimated because GC signals of the substrates, products, or isomers overlapped with the very large peaks corresponding to solvents. ^b Average nanoparticle sizes in catalysts A and D are 2.2 and 3.4 nm, respectively. ^c Initial concentration of K₂PdCl₄ in the PAA deposition solutions.

Table 7. TOFs and TOF Ratios for Unsaturated-Alcohol Hydrogenation Catalyzed by [PAA–Pd(0)/PEI]₃ Films That Contain Pd Nanoparticles with Different Diameters (catalytic films were deposited on micrometer-sized alumina; values in parentheses are the sum of TOFs for hydrogenation and isomerization)

Catalysts	TOFs (moles hydrogenated/ mol Pd/ h) ^{a,b}			
				
	4	5	6	7
Catalyst A ^c [Pd(II)]=1 mM ^d	290±10 (450±10)	150±30 (-)	27±3 (-)	8±2 (-)
Catalyst D ^c [Pd(II)]=15 mM ^d	895±45 (2175±65)	760±10 (-)	233±2 (-)	130±10 (150±5)

^a 25 mM substrate was hydrogenated in 3:1 water:ethanol. TOFs are initial values determined at conversions less than 50%. ^b In some cases, the TOF for the sum of hydrogenation and isomerization was not estimated because the amount of isomer detected was negligible. ^c Average nanoparticle sizes for catalysts A and D are 2.2 and 3.4 nm, respectively. ^d Initial concentration of K₂PdCl₄ in the PAA deposition solutions.

that for **6**, which contains a disubstituted double bond. Interestingly, using the smaller nanoparticles, the TOF for hydrogenation of **5** is 11-fold lower than that for hydrogenation of **1** in 3:1 water:ethanol. This suggests that when using the smaller nanoparticles rates are affected by addition of a bulky substituent α to the double bond, which is consistent with previous studies.²⁴ However, even with **5**, hydrogenation using catalyst A is much faster than with the di- and trisubstituted compounds **2**, **3**, **6**, and **7**. In contrast, catalyst D, which has much larger nanoparticles, shows little difference in the TOFs among the molecules containing monosubstituted double bonds (**1**, **4**, and **5**). Furthermore, selectivities for hydrogenation of **4** and **5** vs di- and trisubstituted double bonds (**6** and **7**, respectively) are much smaller when using the larger nanoparticles in catalyst D than when using catalyst A.

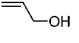
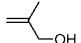
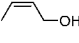
Possible Explanations of Selectivity. The above data demonstrate that selectivity in hydrogenation varies greatly with particle size, and related studies of nanoparticle reactivity imply that

such trends may arise from geometrical effects.⁴⁰ Doyle et al. suggest that the sensitivity of catalytic hydrogenation rates to nanoparticle size occurs because the reaction takes place on specific types of atoms that are more (or less) prevalent on small particles.² Large particles mainly contain terraces with atoms of high coordination numbers, whereas small particles contain comparatively high numbers of surface atoms with low coordination numbers (edge and corner atoms). A recent study based on STM images shows that Pd nanoparticles with diameters < 4 nm are highly defective, whereas nanoparticles with diameters > 4 nm start to develop large and well-defined facets.^{21,41} Several recent studies show that interactions of alkenes with catalysts change with alkene size, and hydrogenation of higher

(40) Bond, G. C. *Surf. Sci.* **1985**, *156*, 966–81.

(41) Freund, H. J.; Baumer, M.; Libuda, J.; Risse, T.; Rupprechter, G.; Shaikhutdinov, S. *J. Catal.* **2003**, *216*, 223–235.

Table 8. TOFs and TOF Ratios for Competitive Unsaturated-Alcohol Hydrogenation Catalyzed by [PAA–Pd(0)/PEI]₃ Films That Contain Pd Nanoparticles with Different Diameters (catalytic films were deposited on micrometer-sized alumina; values in parentheses are the sum of TOFs for hydrogenation and isomerization)

Catalyst	Average nano-particle diameter (nm)	TOFs (moles hydrogenated/ mol Pd/ h) ^a			Ratio of TOFs	
		 1	 2	 3	1/2	1/3
Catalyst A [Pd(II)]=1 mM ^b	2.2	2840±60 (3780±70)	17±5 (45±15)	-	170 (84)	-
Catalyst A [Pd(II)]=1 mM ^b	2.2	3000±200 (3800±150)	-	100±10 (110±10)	-	30 (35)
Catalyst C [Pd(II)]=8 mM ^b	3.2	1550±240 (2340±200)	24±10 (230±20)	-	65 (10)	-
Catalyst C [Pd(II)]=8 mM ^b	3.2	1120±120 (1800±200)	-	85±10 (140±25)	-	13 (13)

^a A 50 mL amount of 25 mM of both substrates was hydrogenated in water. TOFs are initial values determined at conversions less than 50%. ^b Initial concentration of K₂PdCl₄ in the PAA deposition solutions.

alkenes such as *trans*-2-pentene takes place on face atoms.^{2,5,43} Hence, one explanation of selectivity might be that monosubstituted double bonds react primarily at defect sites whereas disubstituted double bonds react primarily on terraces.

Using the Van Hardeveld and Hartog statistics we calculated the number of different types of surface atoms on cuboctahedral Pd nanoparticles containing the same number of atoms as average nanoparticles in catalysts **I**, **J**, **K**, and **L** (nanoparticles suspended in polyelectrolyte solutions) (Table S-2, Supporting Information).^{1,42} Figure S-10, Supporting Information, presents the calculated percentage of surface, defect (edge and corner), and face atoms with respect to the total atoms for each average particle size and shows that the percentage of face atoms changes minimally (from 26% to 20%) as the average particle size increases from 2.6 to 5.1 nm. However, the percentage of defect atoms decreases from 18% to 5% as the average particles size increases from 2.6 to 5.1 nm. Considering, the data for allyl alcohol hydrogenated by suspended nanoparticles (Table 5), on going from an average particle diameter of 5.1 nm to a diameter of 2.6 nm the TOF increases by a factor of 4.2. If reaction only occurs at defect sites and rates per defect atom are independent of particle size, the Van Hardeveld and Hartog statistics would suggest an increase in TOF of 3.6, which is within the experimental error of the measured change. In the case of **2** and **3**, TOFs decrease by a factor of ~2.6 as the size of the nanoparticles suspended in solution (Table 5) decreases from 5.1 to 2.6 nm. This is inconsistent with the fraction of face atoms increasing from 20% to 26% as the nanoparticles size decreases from 5.1 to 2.6 nm. Thus, one would have to assume that the reactivity of terrace sites increases as the terrace size increases, perhaps for steric reasons.

We performed competitive hydrogenations to investigate whether monosubstituted and multisubstituted compounds are hydrogenated on the same or different sites. A large decrease in the rate of hydrogenation of **2** or **3** due to the presence of **1** would suggest hydrogenation on the same sites. Mixtures of either **1** and **2** or **1** and **3** were hydrogenated with catalyst A and catalyst C under the same conditions used in the single-

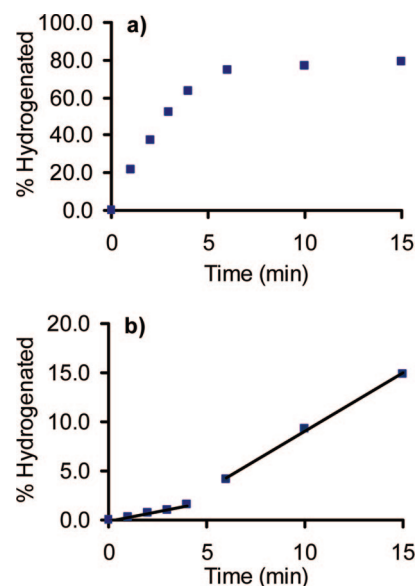


Figure 5. Percent hydrogenation of (a) **1** and (b) **2** during competitive hydrogenation of these substrates using catalyst C. Each substrate had an initial concentration of 25 mM in the mixture. After 6 min, **1** was completely consumed due to hydrogenation and formation of ~20% propionaldehyde. In the bottom plot, lines represent fits to the data before and after complete reaction of **1**.

substrate hydrogenations. Comparison of Tables 8 and 2 shows that TOFs and selectivities obtained with catalyst A are similar in mixtures and single-component systems. However, the large differences in hydrogenation rates between **1** and **2** or **3** make it difficult to see if **1** is reacting at different active sites than **2** or **3** because **1** is rapidly consumed in these reactions and the hydrogenation rates for **2** and **3** are difficult to determine at short times. In contrast, with catalyst C the initial TOFs of **2** and **3** decrease by a factor of ~7 in the presence of **1**, so selectivities are much higher in competitive hydrogenations (Table 8) than in the comparisons of single-substrate experiments in Table 2. Furthermore, after the majority of **1** reacts, the rate of hydrogenation of **2** or **3** increases to values similar to those in the single-substrate experiments (Figures 5 and S-11, Supporting Information). This suggests that **1**, **2**, and **3** react at the same active sites and that the monosubstituted double bonds

(42) Van Hardeveld, R.; Hartog, F. *Surf. Sci.* **1969**, *15*, 189–230.

(43) Stacchiola, D.; Burkholder, L.; Tysoe, W. T. *Surf. Sci.* **2003**, *542*, 129–141.

in **1** are able to bind more strongly to the surface than the multisubstituted double bonds of **2** or **3**. Thus, the enhanced selectivity observed with smaller particles is likely due to weaker binding of **2** and **3** as the particle size decreases and not to binding at different sites. This could be due to more steric hindrance from surrounding polymer as the particle size decreases or electronic effects.

Conclusions

Selectivity in the hydrogenation of monosubstituted over disubstituted double bonds increases dramatically as the diameter of catalytic nanoparticles decreases, and this size-dependent selectivity occurs with both suspended nanoparticles and nanoparticles deposited on micrometer-sized alumina. High selectivities stem from the fact that TOFs for the hydrogenation of monosubstituted double bonds decrease as particle size increases, whereas the TOFs for hydrogenation of multisubstituted double bonds show the opposite trend. When using the smallest nanoparticles (average diameters of 2.2 nm), these trends result in selectivities > 100 for hydrogenation of monosubstituted over

disubstituted double bonds. Selectivities might occur because relative to monosubstituted double bonds multiply substituted double bonds bind less strongly to the more hindered active sites of the smaller nanoparticles.

Acknowledgment. We thank the American Chemical Society Petroleum Research Fund and the National Science Foundation (OIS 0530174) for funding this work. We are grateful to Dr. Jorge Macanás (Université Paul Sabatier) for helpful discussions.

Supporting Information Available: Additional TEM images and histograms of nanoparticle sizes, formulas for Van Hartevelde and Hartog statistics of atom types on particles, estimations of the percentages of large particles and nanoparticles in catalysts **D** and **H**, a graph showing the fraction of different atom types as a function of particle size, and data for competitive hydrogenation of **1** and **3**. This material is available free of charge via the Internet at <http://pubs.acs.org>.

JA807415K